DOI: https://doi.org/10.36094/sc.v89.2025.A_Comprehensive_Review_in_Ultrasonic.Kumar.104

ARTICLE

Sci. and Cult. 91 (1–2) : 104-116 (2025)

A COMPREHENSIVE REVIEW IN ULTRASONIC NON-DESTRUCTIVE TESTING AND EVALUATION FOR CARBON FIBRE REINFORCED PLASTICS STRUCTURES

M. RAMESH KUMAR, AMITABHA DATTA* AND V. SRINIVASA

In ensuring quality control and assessing the safety and reliability of Carbon Fibre Reinforced Plastics (CFRP) aircraft structures, it is imperative to detect any damage or defect across various stages, spanning from production to operational use. This paper delineates the research undertaken by the Advanced Composites Division (ACD) of CSIR-National Aerospace Laboratories (CSIR-NAL) concerning the diverse applications and scenarios wherein ultrasonic Non-Destructive Testing and Evaluation (NDTE) is applied to composite aircraft structures. CFRP laminates, incorporating simulated defects, impact damage, and structures from the home-built SARAS aircrafts, underwent ultrasonic inspection. The inspection observations were compared with through transmission (single-element water squirter systems), linear array pulse echo (roller probe systems), and air-coupled non-contact ultrasonic system in terms of their accuracy and found good correlation with ground truth.

Keywords: *Air coupled ultrasonic, Carbon fiber reinforced plastic, Defect detection, Through transmission, Pulse echo.*

Introduction

Use of composite materials in primary aircraft structures has been steadily increased in the last few decades. Presently, as much as 53% structural weight of A350 commercial aircraft is from composite materials[1]. Light Combat Aircraft (LCA) Tejas, indigenously designed and developed in India contains more than 45% of composite materials by weight. Next generation aircrafts are expected to have highly integrated co-cured composites in their primary load-bearing structures. Despite the inherent advantages such as high stiffness-to-weight ratio, excellent strength and corrosion resistance, low weight of the composite structures, they are more prone to have damages like disbond or delamination, leading to potential threat to the structural integrity[2-3]. In the context of ensuring quality control and assessing the safety and integrity of aircraft structures, it is imperative to detect damage at various stages, spanning from manufacturing to operational service. Furthermore, major threat during operational life of the composite aircraft structure is the barely visible impact damage (BVID), which can occur due to tool drop, runway debris, ground vehicle impacts, *etc.*[4]. Such events on composite structures can leave sub-surface damages which are not visible to naked eyes during routine inspections. Such damages are known to reduce load-carrying capacity of structures, hence compromise safety of the aircraft.

Several reputed research groups have extensively investigated damage or defect in composite structures using diverse methodologies, including X-ray testing[5-8], optical testing[9-12], magnetic particles testing[13], infrared thermography[14-17], ultrasonic testing (UT)[18-23], eddy current

Advanced Composites Division, CSIR-National Aerospace Laboratories, Bengaluru 560017, India

* Corresponding Author: amitabha@nal.res.in

testing [24-25], electromagnetic testing (ET)[26], acoustic emission (AE)[27], shearography[28]. Further, relevant literature on Non-Destructive Testing and Evaluation (NDTE) techniques used for Carbon Fiber Reinforced Plastic (CFRP) structures can be found by referring to the cited literature[29-31].

Notably, ultrasonic inspection emerges as a highly reliable and effective technique for evaluating structural integrity[32]. Its capability to scan the cross-sectional area of structures renders it particularly advantageous for identifying damage in advanced composite materials. Moreover, ultrasonic testing offers portability, cost-effectiveness, and improved scanning speed and resolution, contributing to its widespread application. Ultrasonic waves travel through composite materials and provide details about the interface between the base material and any discontinuities. This allows the detection of defects by determining their location, size, and direction. The ultrasonic through transmission method is a useful tool for monitoring transmission losses resulting from delamination and disbonds, as well as for detecting volumetric defects such as voids in composite structure. This approach is effective for both low energy and high energy impacts. Furthermore, linear array pulse echo system provides real-time display of A, B, and C-scans. The high-resolution C-Scan displays either time of flight or amplitude data. The data is shown in a two-dimensional format, showing a plane view of the test structure. The colour map indicates the depth or amplitude of the gated signal at each place in the test component, corresponding to its position.

This paper provides a concise summary of the extensive research conducted by CSIR–NAL on the use of ultrasonic non-destructive testing and evaluation for composite structures and the organization of the paper is as follows: Sec. 2 outlines the testing methodology, which primarily includes through transmission (single element water squirter technique), pulse echo/time of flight (linear array roller probe technique), and air-coupled non-contact ultrasonic technique. Sec. 3 provides an overview of the inspection results and discussion. Sec. 4 focuses on the development of AI-driven automated defect detection software using the ultrasonic data. Sec. 5 then explores the challenges and opportunities in the field of ultrasonic systems followed by conclusion in Sec.6.

Ultrasonic Testing Methodology for Composites

Ultrasonic testing indeed relies on piezoelectric transducers to generate compression or shear waves that propagate through the material being inspected. These waves interact with boundaries within the material, leading to reflection, transmission, and scattering. These interactions, along with the speed of sound and travel time, offer insights into the material's properties and integrity. In ultrasonic inspection of composites, the sound beams travel in a path parallel to the reinforcing fibres. This allows for efficient characterization of faults such as fiber misalignment. Delamination and fibre de-bonding can result in a distinct reflection, as well as a decrease in transmission, from a specific depth within the material. As a result, they can be reliably recognized with a high level of confidence. Porosity does not generate a distinct reflection, but instead disperses the ultrasonic waves, leading to a loss of transmission that can be accurately described as outlined. Our studies have also indicated that the reduction of waves traveling at a right angle to CRFP layers could offer valuable insights for identifying and understanding the quality between layers. To enhance the likelihood of detecting defects and accurately pinpointing their location, a range of signal processing techniques in both the time domain and frequency domain are employed. These approaches help differentiate the echoes produced by defects from the many waves that bounce off the surfaces of CFRP structure. Within our division, we have employed a ten axes ultrasonic C-Scan system, a pulse-echo linear array roller probe system, and an air-coupled ultrasonic system. These facilities are utilized for ultrasonic Non-Destructive Testing and Evaluation (NDTE), with further details provided below.

Conventional Ten Axes Ultrasonic C-Scan System: A state-of-the-art multi-axes single channel ultrasonic C-Scan system from ScanMaster[33] has been set up at ACD illustrated in Fig. 1. The system is equipped with a pair of water squirters and a 10-axes probe manipulation facility. The system, equipped with drive-on and drive-off capabilities, has an inspection chamber measuring 9 meters in length, 3 meters in width, and 1.2 meters in height. The 10-axes probe manipulation facility enables the examination of composite structural components with intricate curves and geometry. Additionally, it is capable of acquiring and displaying ultrasonic data in real time using via transmission amplitude, pulse echo amplitude, and time-of-flight. This can be done individually through separate scans or simultaneously in a single scan. Image enhancement and analysis software packages are used to conduct thorough examination of the recorded data.

Pulse Echo Linear Array Roller Probe System: The linear array roller probe, Rapid Scan system from Sonatech[34] illustrated in Fig. 2 is equipped with advanced

(a) (b)

Fig.1: (a) Ten-axes computer-controlled ultrasonic C-scan system with inspection envelope measuring 9 m in length, 1.2 m in width, and 3 m in height. (b) Conventional squirter unit.

Fig. 2: Pulse echo linear Array Roller Probe (Rapid Scan System)deployed at CSIR-NAL

features that allow for simultaneous live A, B, and C-scans, facilitating comprehensive inspections across large areas. This capability is particularly beneficial for identifying defects or anomalies in carbon composite laminates and other structural materials. Post-inspection data processing is carried out using full waveform capture, ensuring detailed analysis and accurate defect characterization. The pulsar type utilized in the system is a negative square wave, delivering a consistent amplitude of 70 V. This waveform is optimized for generating precise and reliable ultrasonic signals. The pulse width can be adjusted between 25 ns to 250 ns, offering flexibility to adapt to various testing requirements and material types. With 32 active channels as a standard configuration, the system provides a robust foundation for inspections. Additionally, it can be expanded to accommodate up to 128 channels, allowing for increased versatility and

(a) (b)

Fig. 3: (a) Air-Coupled Ultrasonic System Featuring a Controller, Scanning Area, and Transducer Holders(b) Image of the System Deployed at CSIR–NAL

coverage. The system's wide bandwidth, ranging from 1 MHz to 22 MHz, ensures high-resolution imaging and detection capabilities. The receiver gain is set at 80 dB, enhancing the system's sensitivity and enabling the detection of subtle defects or discontinuities. Multiple centre frequencies are available, including 2, 5, and 10 MHz, catering to different inspection needs and material thicknesses. Furthermore, the system features an element pitch of 0.8 mm, ensuring precise spatial resolution. The active array width is designed to cover 50 mm, striking a balance between coverage and resolution for efficient inspections.

These specifications collectively contribute to the system's capability to provide accurate, reliable, and detailed inspection results for a wide range of applications in the aerospace and composites industries.

Air Coupled Ultrasonic System: Air-coupled ultrasonic testing is an advanced non-contact technique suitable for inspection of composite materials, characterization of their internal structure, and detection of defects. Unlike conventional contact-based ultrasonic methods that utilize a liquid couplant for transducer coupling to materials, air-coupled testing employs air as the coupling medium. This method utilizes specialized air-coupled ultrasonic transducers equipped with piezoelectric elements that convert electrical energy to mechanical vibrations and vice versa.

The air-coupled ultrasonic testing method offers several significant advantages. Firstly, it enables non-contact inspections, eliminating the necessity for direct surface coupling. This makes it particularly suitable for inspecting irregular or delicate surfaces without the risk of damage. Secondly, it allows for rapid and efficient inspection of large composite structures, such as aerospace components or wind turbine blades, reducing the need for extensive surface preparation or couplant application, leading to time and cost-effectiveness. Additionally, the method aids in material characterization by deriving mechanical properties such as wave velocities and attenuation, which can be correlated with parameters like density, stiffness, or elastic moduli, thereby enhancing our comprehension of composite materials' behaviour and integrity. The air-coupled system developed by The Ultran Group[35] represents a precise tool for damage detection in a broad spectrum of materials across various industries, as illustrated in Fig. 3. This system comprises a fully equipped ultrasonic analysis system capable of both internal and surface imaging. It facilitates the investigation of defects, heterogeneity, delamination, porosity, velocity/density, thickness, and Time of Flight measurements.

Results and Discussion

In this section, we present the results of ultrasonic inspection conducted on CFRP laminates, which included simulated defects, impact damage, and structures from home-built SARAS aircraft.

CFRP Laminate with Simulated Defect: The CFRP Laminate, with a cross section measuring 300 mm ´ 300 mm ´ 6 mm, is manufactured with twelve simulated defects of varying sizes. These defects are created using diverse materials such as bagging film, blade pieces, flash breaker peel ply, release film, and Teflon film. The defects are placed at different depths between the plies, as shown in Fig. 4a. Ultrasonic non-destructive evaluation (NDE) techniques are essential for assessing the quality of the laminate and detecting any defects that might be present. As mentioned earlier, we utilized a through transmission and linear array roller probe equipment to assess the laminate. The through transmission C-Scan examination provides a visual representation of the relative distribution of attenuation in a component, displaying a planar view perspective of the component. The defects exhibit a comparable arrangement with significant degrees of attenuation in contrast to the original structure.

This attenuation is quantified in terms of energy loss in the component, measured in decibels (dB). The C-Scan map of a simulated defect laminate obtained using conventional ultrasonic through transmission examination is illustrated in Fig. 4b.

In the process of through transmission inspection, we used a probe frequency of 5 MHz, a Teflon holder diameter of 6 mm, and a scan speed of 70 mm/sec, with grid sizes of 1 mm. As mentioned previously, the linear array roller probe system provides real-time display of A, B, and C-scan. The high-resolution C-Scan displays either time of flight or amplitude data. The data is shown in a two-dimensional format, showing a plane view of the test structure. The colour map indicates the depth or amplitude of the gated signal at each place in the test component, corresponding to its position. The time of flight or pulse echo map of the laminate shown in Fig. 4c was obtained using linear array rapid scan examination. It is evident that the image seen in Fig. 4c comprises of seven individual image files, which are combined during post-processing to create the final image. A comparison is made between the dimensions of the defect for both procedures and the actual

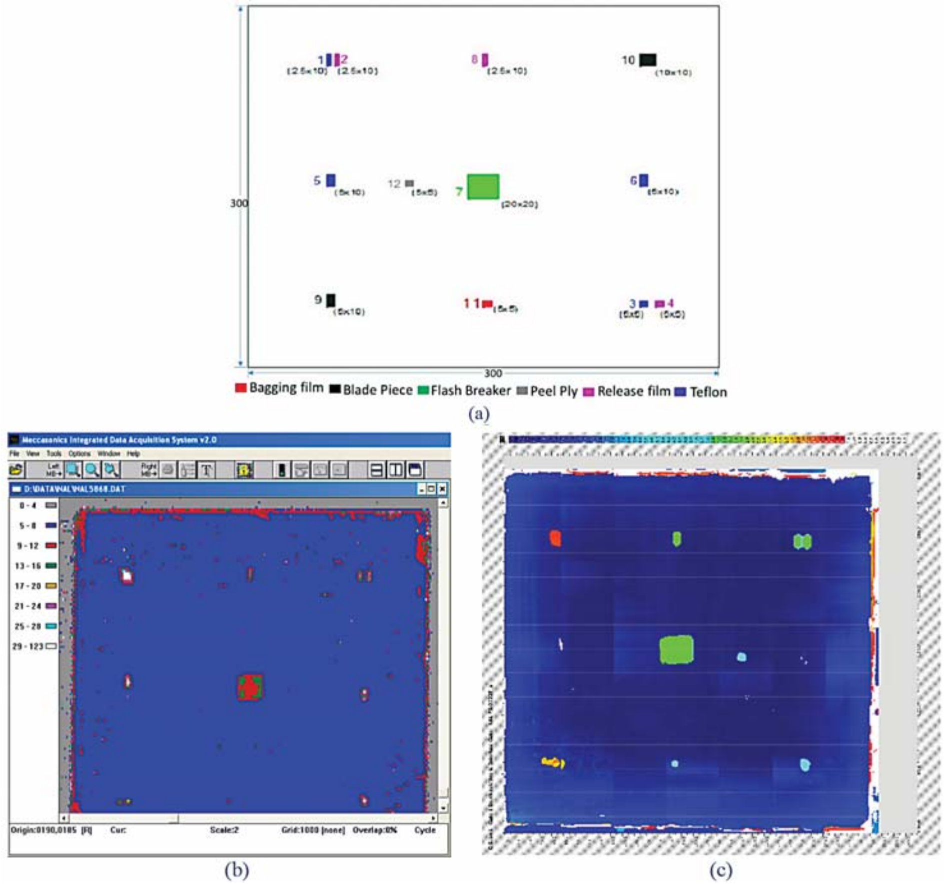

Fig. 4: (a) The CFRP laminate of cross section of 300 mm x 300 mm x 6 mm fabricated with 12 simulated defects of different size using various materials located at various depths between the plies (b) Conventional through transmission C-Scan map (flip Fig. 4a by 180^{o}) (c) Pulse echo linear array Rapid Scan Plot (flip Fig. 4a by 180^{o})

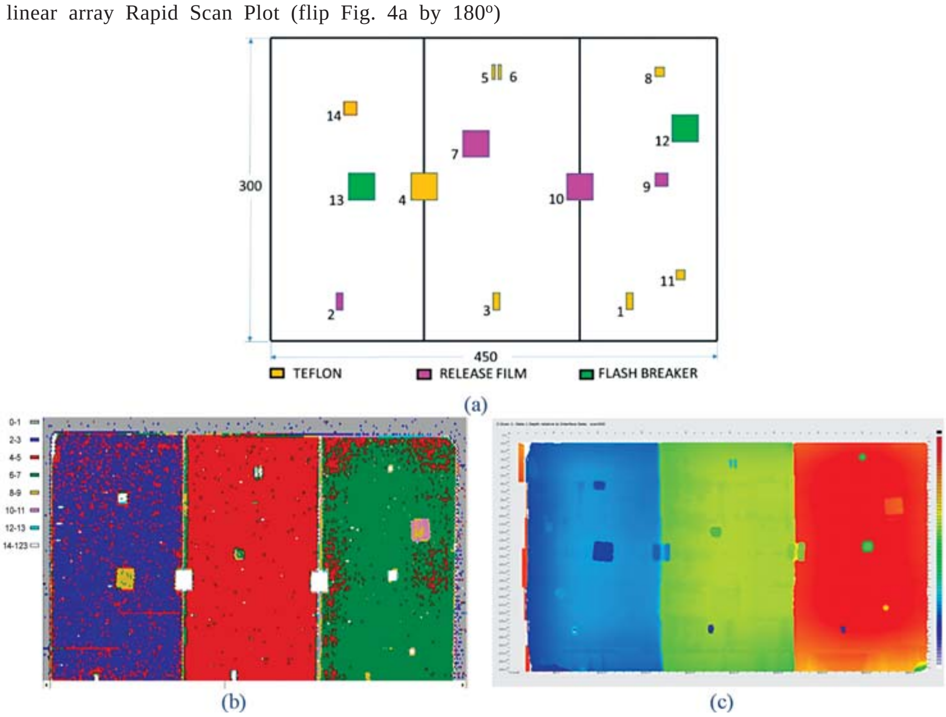

Fig. :. (a) The CFRP stepped laminate of cross section of 450 mm x 300 mm of variable thickness from 2.25 mm, 4.5 mm, 6.75 mm fabricated with 14 simulated defects of different size using various materials located at various depth between the plies (b) Conventional through transmission C-Scan map (c) Linear array time of flight roller probe system.

damage, and the results are shown in Table 1. Within the through transmission approach, the maximum error is 20 mm^2, whereas within the linear array roller probe system, the maximum error is 41 mm^2 and maximum depth error is 1.3 mm^2.

CFRP Varying Thickness Laminate with Simulated Defect: Similarly, another CFRP stepped laminate with a cross section of 450 mm x 300 mm and a variable thickness ranging from 2.25 mm to 6.75 mm was manufactured with 14 programmed defects of varying sizes utilizing a variety of materials situated at various depths between the plies and illustrated in Fig. 5a. Our evaluation of the laminate's quality was accomplished through the utilization of both the through transmission method and the linear array roller probe system. Figure 5b illustrates the C-Scan map of a laminate with a variable thickness that was acquired by transmission examination utilizing conventional ultrasonic techniques and Fig. 5c illustrates the linear array time of flight Rapid Scan map utilized for the same laminate. Additionally, a comparison is done between the dimensions of the defect for both procedures and the ground truth, and the findings are presented in Table 2. Within the through transmission method, the maximum error is 62 mm^2, whereas within the linear array roller probe system, the maximum error is 62 mm^2 and the maximum depth error is 0.2 mm^2. As can be seen

Table 1: Comparison of actual dimenson and measured dimension of simulated defect laminate

Defect ID	Actual dimentions		Mesured Dimentions		
			Through Transmission C-Scan	Linear array roller probe	
	Defect size (mm^2)	Depth of (Defect (mm)	Defect size (mm^2)	Defect size (mm^2)	Depth of defect (mm)
1	2.5 × 10	3.45	3 × 10	3 × 10	3.53
2	2.5 × 10	3.45	3 × 10	3 × 10	3.5
3	5 × 5	4.65	5 × 5	5 × 5	4.75
4	5 × 5	4.65	5 × 5	5 × 5	4.7
5	5 × 10	0.15	5 × 11	5 × 10	0.9
6	5 × 10	6.6	5 × 10	5 × 11	6
7	20 × 20	3.6	21 × 20	21 × 21	3.63
8	2.5 × 10	3.6	4 × 10	2.5 × 10	3.68
9	5 × 10	2.4	6 × 10	3 × 10	3.7
10	10 × 10	5.4	10 × 10	12 × 10	5.56
11	5 × 5	2.4	5 × 5	5 × 5	2.57
12	5 × 5	2.4	5 × 6	6 × 7	2.5

Table-2: Comparison of actual dimenson and measured dimension of varying thickness laminate

Defect ID	Actual dimentions		Mesured Dimentions		
			Through Transmission C-Scan	Linear array roller probe	
	Defect size (mm^2)	Depth of Defect (mm)	Defect size (mm^2)	Defect size (mm^2)	Depth of defect (mm)
1	5 × 10	0.15	6 × 11	5 × 9	0.9
2	5 × 10	0.15	5× 10	4 × 9	0.9
3	5 × 10	0.45	6 × 10	6 × 10	0.9
4	20 × 20	1.95	19 × 20	20 × 21	2
5	2.5 × 10	2.1	3 × 10	2 × 9	2.42
6	2.55 × 10	2.1	3 × 10	3 × 9	2.42
7	10 × 10	3.15	11 × 12	11 × 11	3.28
8	5 × 5	3.15	6 × 6	5 × 5	3.23
9	10 × 10	3.15	11 × 11	11 × 10	3.34
10	20 × 20	4.2	20 × 21	20 × 20	4.56
11	5 × 5	5.4	6 × 6	5 × 6	5.51
12	20 × 20	6.15	21 × 22	21 × 21	6.1
13	20 × 20	0.9	20 × 22	21 × 22	1.07
14	10 × 10	1.65	11 × 10	10 × 9	1.77

from Tables 1 and 2, the defect that is located at a depth of 0.15 mm is displaying a depth of 0.9 mm from the roller probe scan data. This is due to the fact that the system has a resolution of 0.9 mm, which means that any defect that is below, in this case 0.15 can't be identified by the system effectively, and it will display 0.9 mm.

Laminate with Barely Visible Impact Damage: The barely visible impact damage (BVID) is a major concern for composite structures during the service. Here we have investigated CFRP composite laminate which is subjected to low-velocity impact tests using a drop weight tower. The selection of laminate thickness and ply layup sequence for this study is based on the layup sequence employed in the top and bottom skin of the structural components. The laminate is clamped all around the edges leaving an unsupported window of 125 mm by 75 mm and the impact is done at the centre of the laminate, manifested BVID. A range of impact energy levels, namely 2, 3, 6, 9, 17, 20, 25, 30, 40, and 50 J, were systematically employed. These impact energy levels were precisely applied to a set of seven distinct laminate thicknesses, specifically measuring 1.36, 2.38, 3.06, 3.74, 4.76, 6.46, and 8.84 mm. A comprehensive series of 98 impact experiments were systematically carried out for this study. Following the creation of BVIDs at the centre of the laminate, a comprehensive assessment was conducted on all laminates by subjecting them to a rigorous examination utilizing through transmission as well as pulse echo linear array roller probe. The purpose of this assessment was to investigate and characterize the extent and nature of the damage induced at the centre of the laminate due to the BVID. By using a 5 MHz probe frequency, which is well-suited for such type of inspection, we were able to obtain detailed information about the damage, including its size, location, and depth.

For illustrative purposes, a laminate with thickness of 4.76 mm was selected from 98 impact experiments as mentioned earlier, and 30 J energy was used to induce BVID. Figure 6a illustrate a conventional through transmission C-Scan map, while Fig 6b shows a linear array roller pulse echo inspection results / mapping. It is evident from Fig. 6a that the conventional through transmission image solely depicts the outer boundary (area) of the damage caused by BVID. In contrast, the roller probe image in Fig.6b, not only reveals the damage boundary but also provides information about the depth of the damage.

T-Section Panel: In conventional through transmission C-Scan inspection of T-Section, the flange and web regions can be scanned individually, but the web flange junction cannot be investigated using through transmission mode due to the inaccessibility of the probe. The linear phase roller probe allows for independent inspection of both the web and flange, including the acquisition of data at the junction between the two without significant challenges. Two defects are introduced at the junction of the web and flange in the centre of the web in this specific T-Section reference panel, as shown in Fig. 7a. The web flange junction exhibits satisfactory consolidation, with the exception of two defects illustrated in linear array time of flight roller probe Rapid Scan Map Fig. 7b. However, the majority of the signals disperse due to the inherent properties of this specific area. Any observable sign in this intersection will unequivocally indicate that the level of consolidation needs to be questioned. The position, intensity, and extent of the echo/ signal will determine the specifics of the problem. Assessing the structural integrity, particularly at the web flange junction, is a challenging task in traditional pulse echo A-Scan examination. The roller probe system is highly effective due to its ability to collect data over a wide inspection area. It also allows for easy programming, storage, and retrieval of test parameters. This enables inspection, comparison with previous references, and multiple inspections using the same parameters.

Torsional Box of SARAS Aircraft: Thus far, our discussion has centred on structures with relatively simpler geometries. Now, we will shift our focus to the inspection of structures characterized by more intricate geometries. Such structure is the torsional box with co-cured construction. The two skins and ribs together co-cured with multi-spar (6 nos. shown in C-Scan map in Fig.8b). The Fig. 8a illustrated the torsional box fabricated at ACD. The entire box is made as a single piece in one operation. To fabricate the co-cured box tubular vacuum bags are used. The tooling for this component includes a set of internal tools and a set of locating tools. The outer mould along with the skin lay-up is placed on the spar and mid rib layup and the entire assembly is under vacuum. The structure features with the skins being securely attached to the spars through co-curing during manufacturing. The spars are co-cured with the skins, forming an I-Section. This torsional box must undergo non-destructive inspection to assess the quality of the joints. Due to the box section construction and variable width from 5 mm at the tip side to 20 mm at the root side, non-destructive inspection was challenging in nature. In order to conduct a comprehensive inspection in one pass, water is filled between the skin and performed a through transmission inspection. The C-scan results illustrated in Fig. 8b, indicated that there is variation in thickness from the tip to the root side, which is accurately captured through transmission inspection dB level ranges from 23 to a maximum of 64. The Zone-1 and Zone-2 are designated with increased thickness in order to accommodate the metallic fittings to the aircraft's fuselage. Further, segment scan of tip side of the torsional box using linear array roller probe system is illustrated in Fig. 8c.

Within this particular framework, one can refer to the analogous research carried out by the Silesian University of Technology and the Air Force Institute of Technology in Poland about the vertical stabilizer of the MiG-29 illustrated in Fig. 9[36,37]. Their study used ultrasonic C-Scan techniques to generate planar images depicting transmitted/received wave attenuation and a time-of-flight map. The complexity of barely visible impact damage (BVID) makes the analysis of resulting C-Scan images challenging. Therefore, authors are leveraging image processing techniques to facilitate analysis of the collected images, improving the accuracy and efficiency of damage assessment. It is worth mentioning that we are also facing the similar challenges and to overcome such issues we have developed AI-driven automated defect detection software, details about the same is presented in next section.

AI-Driven Automated Defect Detection Software Development

As industry 4.0 initiatives continue to advance, the mass production of composite structure is poised to integrate Industry 4.0 principles in the foreseeable future.

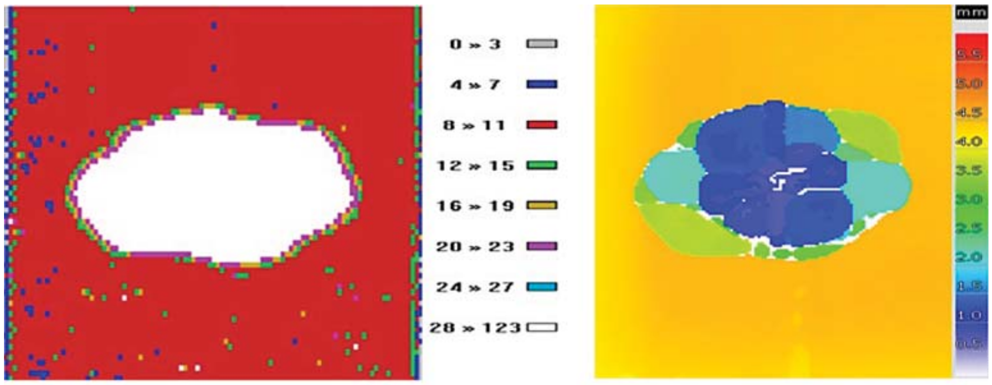

(a) (b)

Fig. 6: A laminate with thickness of 4.76 mm with unsupported window of 125 mm by 75 mm and the impact is done at the centre of the laminate with 30J energy (a) Conventional through transmission C-Scan map (b) Linear array time of flight roller probe Rapid Scan map

Fig. 7: T-Section panel with two defects are introduced at the junction of the web and flange in the centre of the web (b) The web flange junction exhibits satisfactory consolidation, with the exception of two defects (Blue) in Rapid Scan plot

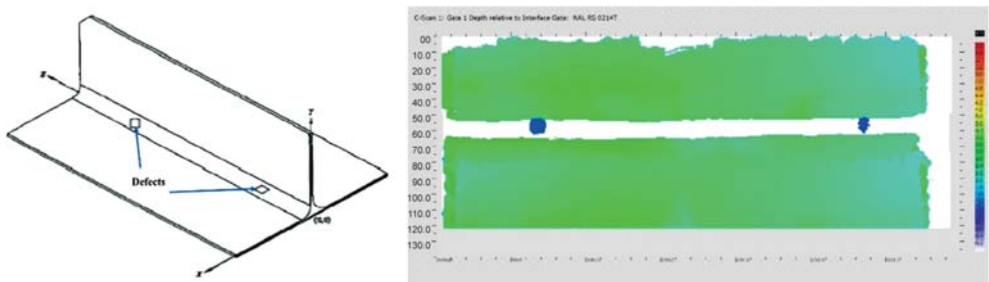

(a) (b)

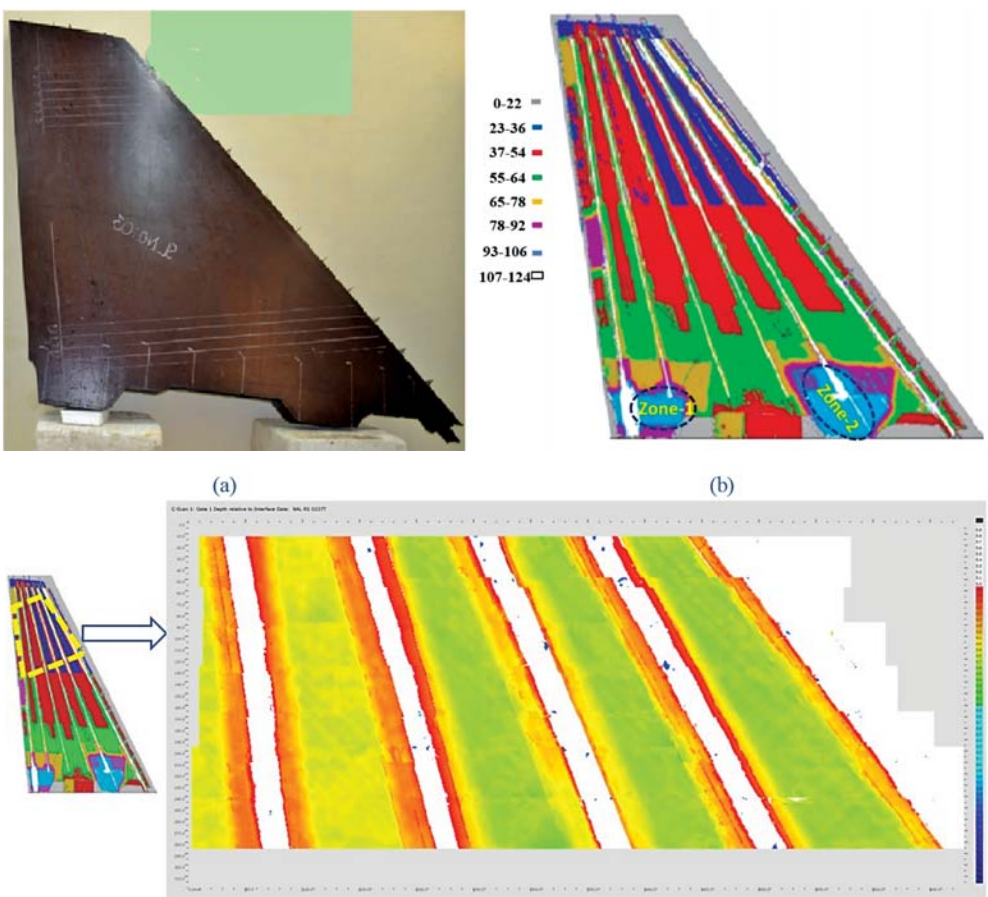

(c)

Fig. 8: (a) The torsional box (Fin of SARAS) is the main load carrying member which is a multi-spar (6 nos.) construction with mid rib and clips fabricated by ACD (b) C-Scan map of through transmission ultrasonic inspection (c) Segment scan of tip side of the torsional box using linear array roller probe system.

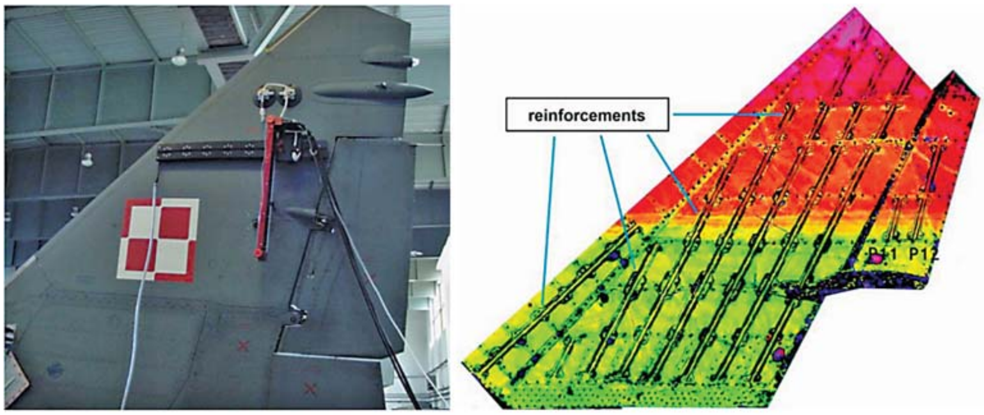

(a) (b)

Fig. 9: (a) MiG-29 composite vertical stabilizer for NDT inspection (b) Time-of-Flight (ToF) C-Scan of the inspected vertical stabilizer[36]

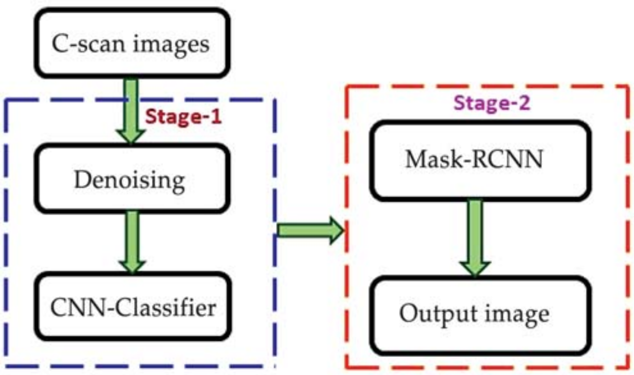

Fig. 10: Flowchart representation of the Software (Model): Classifying C-scan images in the first stage and, when damage is detected, using Mask R-CNN to identify shapes and measure the damage's extent in the second stage

Consequently, conventional NDTE procedures, which rely on human inspectors for decision-making, must evolve towards a future state of fully automated NDE processes, eliminating the need for human intervention[38-39]. In pursuit of this objective, our current focus is on the development of artificial intelligence (AI) driven automated software to estimate damage size using the C-Scan results obtained from the test structure. The objective of this approach was to provide inspectors with the requisite tools to promptly and accurately discern and assess defects in composite materials, with the potential to substantially enhance the efficiency and precision of quality control processes in composite structures.

In order to accomplish this, we implemented a two-step methodology, as illustrated in Fig 10. For more detailed information, please refer to our work cited in reference[40].

In the first stage, as indicated in the flowchart, we performed Convolutional Neural Network (CNN) based classification on the C-scan image of the test laminate. Subsequently, at stage 2, in cases where damage was detected, we utilized Mask R (Recurrent) -CNN on the C-scan images to identify arbitrary shapes and calculate the extent of the damage. The raw C-scan image, initially sized at [1000, 600], was subjected to de-noising (optional) and evaluated by a CNN-based classifier to ascertain the presence or absence of damage in the input image. We opted for a CNN-based Classifier due to its proven ability to accurately recognize damage in images, its capacity to autonomously learn and extract intricate features, and map them to their respective classes, ensuring precise image classification. Furthermore, CNNs exhibit adaptability to diverse damage sizes, scales, and orientations.

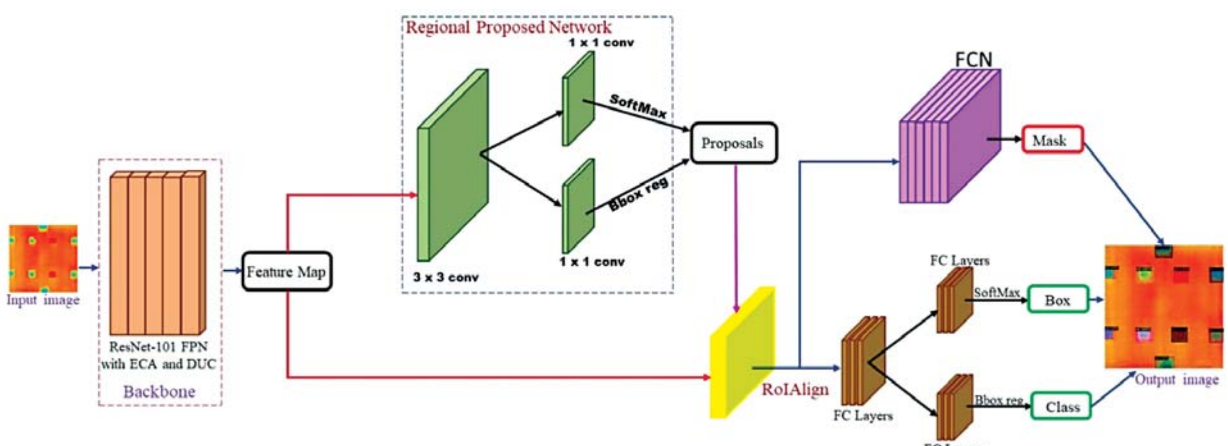

Fig. 11: Mask R-CNN architecture for defect zone bounding boxes and segmentation masks

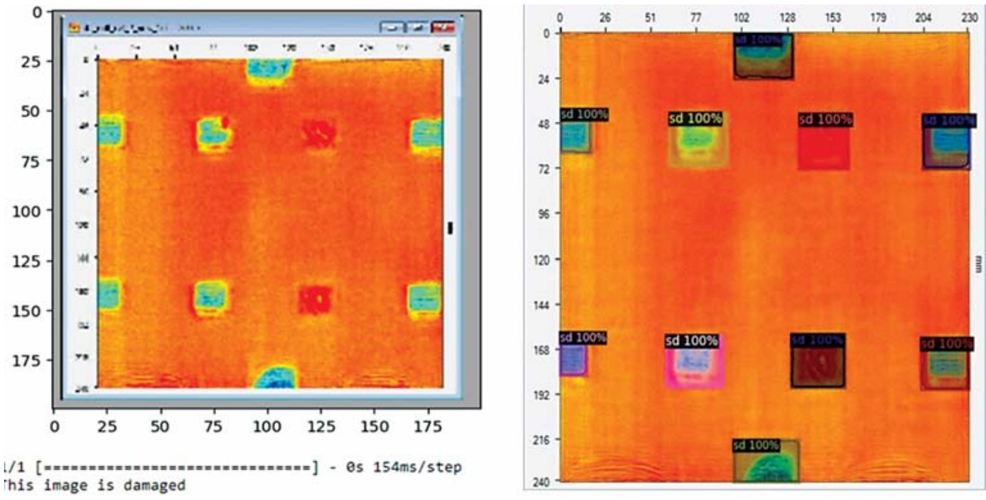

(a) (b)

Fig. 12: (a) CNN Image classifier: Whether the image is damage or not (b) Mask R-CNN: Creates a mask over the damage area

After damage has been classified, the input image is first passed through a backbone network, which is typically a deep convolutional neural network (CNN) like ResNet-101(Residual Neural Network) and Feature Pyramid Network (FPN) architecture. The backbone network extracts a set of feature maps at different scales, representing features from low-level edges and textures to high-level object and context information as illustrated in Fig. 11.

In this study, we present two key outcomes. First, we describe the outcome of the classification process conducted using a CNN-Classifier implemented through Keras illustrated in Fig. 12a. Subsequently, performance of the Mask R-CNN algorithm illustrated in Fig. 12b, which was initially trained to detect various defects and shapes based on specific detection requirements. The model demonstrated satisfactory performance across most detection tasks. Pre-trained weights are available for the Mask R-CNN model and can be utilized for defect detection, with the option to update these weights during subsequent model training. To refine the model's ability to identify objects and shapes, we conducted further training using our dataset that included various shapes. The model underwent training and validation testing, achieving a mean Average Precision (mAP) of 89% after 1000 epochs. The validation loss function plateaued at 0.004, while accuracy consistently remained around 0.988 for our dataset. These findings demonstrate the model's capacity to effectively detect both small, clustered objects within a

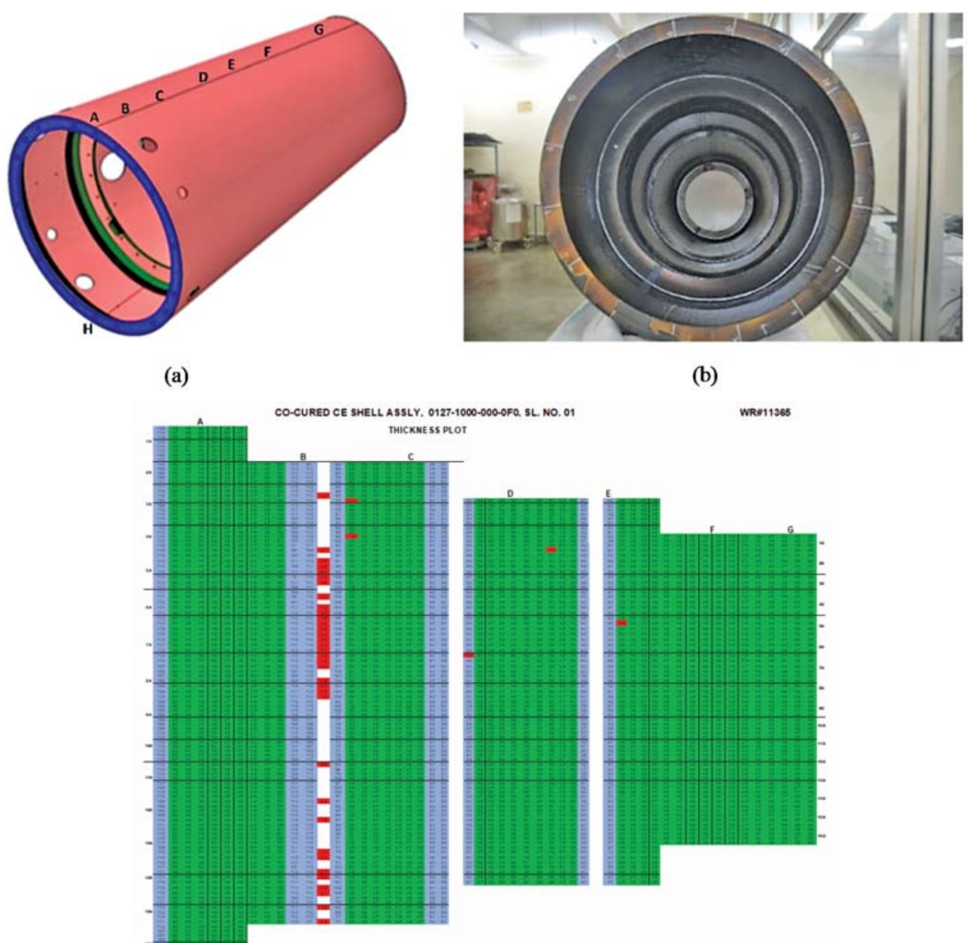

(a) (b) (c)

Fig. 13: (a) CAD model of shell structure comprised of eight different thickness regions (A to H) (b) Pictorial representation of the structure (c) Manually inspected A- Scan map

single image and larger or medium-sized objects in an image.

This cost-effective design will encourage the Indian industry to use the software for their NDT &E application. Several industrial partners, including HAL and DRDO, are in collaboration and commercialization of this software.

Challenges and Opportunities

When dealing with composite materials, conventional ultrasonic methods face challenges due to the anisotropic nature of composites. Anisotropic materials exhibit different properties when measured along different axes, which complicates the interpretation of ultrasonic signals. This complexity arises because the speed of sound and scattering characteristics can vary depending on the direction of propagation relative to the composite's structural orientation. Addressing these challenges typically involves specialized techniques tailored to account for the anisotropic behaviour of composite structures. This may include employing multi-angle inspections, advanced signal processing algorithms, or utilizing specialized transducers designed to accommodate the complex nature of composite materials. By adapting ultrasonic testing methodologies to suit the specific characteristics of composites, engineers and technicians can more effectively assess their properties and integrity.

The primary drawback of the existing C-Scan inspection system lies in its inability to thoroughly inspect the entire surface of a fully circular structure or shell structure as shown in Fig. 13. The system restricts the inspection to only certain areas of the section, leaving other regions unexamined. As a result, potential defects or imperfections outside the cone's coverage may go unnoticed, leading to compromised product quality and safety concerns. The process of qualifying such a structure after production took a total of 80 man-hours. This qualification process likely involved rigorous testing, inspection, and quality assurance measures to ensure that the structure met the required standards and specifications. Now, with the system that we are proposing, there will be a substantial improvement in the qualification process. The man-hours required for qualification are anticipated to reduce by a factor of three. This means that the proposed system is expected to be much more efficient and streamlined in its testing and inspection procedures. In other words, the qualification of the new system is estimated to take only one-third of the time it took to qualify the existing structure. This reduction in man-hours signifies a significant improvement in productivity, allowing for quicker and more cost-effective qualification of the new system while ensuring it meets all necessary quality standards. Especially sandwich foam construction radome structures benefit from such a system.

Researchers are exploring the combination of ultrasonic techniques with other NDTE methods, such as eddy current testing, thermography, and X-ray imaging, to overcome limitations and enhance inspection capabilities. These multi-modal and hybrid approaches offer complementary information for more comprehensive defect assessment. One such example is development of innovative robotic platform for autonomous inspection integrating both infrared thermography (IRT) and phased array (PA) non-destructive evaluation techniques to enhance damage detection and characterization capabilities by Padiyar *et al.*[41]. This advanced system leverages the strengths of IRT and PA methods to provide comprehensive analysis and precise identification of defects in composite in-situ aircraft structure inspection. This dual-technology approach ensures that a wide range of defects can be detected and characterized accurately, enhancing the reliability of the inspection process. The platform's autonomy further increases efficiency, reduces inspection time, and minimizes the risk of human error, making it a valuable tool for maintaining the structural integrity of critical components in various industries, including aerospace, automotive, and civil infrastructure.

Another critical issue with the current inspection system is its lack of ruggedness and the subsequent susceptibility to frequent hardware failures. The delicate nature of the hardware components renders the system prone to communication failure caused between hardware and software. As a consequence, frequent breakdowns disrupt the inspection process, resulting in production delays and increased maintenance costs. The rapid inspection of large aerospace composite structures and commercial composite parts using multi-sensor systems represents a transformative advancement in the aerospace industry. By integrating multiple advanced inspection technologies, this approach streamlines the inspection process, ensuring comprehensive data collection and precise defect detection. The expedited turnaround time enhances productivity and minimizes production disruptions, while the non-destructive testing advantages provide reassurance about the structural integrity of aerospace composites. Embracing this cutting-edge inspection technology will undoubtedly elevate aerospace safety, improve quality assurance, and further solidify the industry's commitment to excellence.

Conclusions

The Advanced Composites Division (ACD) of CSIR–National Aerospace Laboratories has garnered recognition as a Centre of Excellence in Composite Structures by the Aeronautics Research and Development Board (ARDB). Renowned for its contributions to composite structures in both military and civil aircraft, the division is committed to maintaining a leading edge in technology through a blend of fundamental research and practical R&D initiatives. Proficient in design, fabrication, Non-Destructive Testing (NDT), repair, and structural testing, the division offers end-to-end solutions from concept development to certification. It actively pursues research in emerging areas such as Non-Destructive Testing & Evaluation (NDTE), Structural Health Monitoring (SHM), Damage Tolerant Structures, and processing of advanced materials like thermoplastics, 3D-composites, and Nano composites.

Ensuring quality control and assessing the safety and reliability of Carbon Fiber reinforced Plastics (CFRP) aircraft structures require detecting damage or defects at various stages, from production to operational use. This work delves into the research conducted by the Advanced Composites Division on the applications of ultrasonic non-destructive testing and evaluation in composite aircraft structures. Utilizing ultrasonic inspection, a range of carbon composite laminates, including those with simulated defects, impact damage, and home-built aircraft structures, were evaluated. Comparative analyses were conducted with single-element water squirter through transmission ultrasonic systems, linear array pulse-echo roller probe systems, and air-coupled non-contact ultrasonic systems, demonstrating good correlation with ground truth. Further, automated defect detection software integrated with Artificial Intelligence (AI) algorithms, including Convolutional Neural Networks (CNN) and Mask R-CNN are used for defect detection of ultrasonic testing (UT) data. Such an automated approach significantly enhances efficiency and accuracy compared to conventional manual inspection methods.

Acknowledgments

The authors express their gratitude to Mr. Suresh Chand Jangir, Mr. Ajay Kumar, and Mr. S. Kali Kiran from the NDT group, ACD, and also extend appreciation to the former head of the division of ACD, Dr. M.R. Madhava, Mr. H.N. Sudheendra and Dr. Ramesh Sundaram for their invaluable guidance and support.

Also, we would like to thank Mr. Nadeem Masood and Mr. M.J Augustin for reviewing the manuscript.

Further, the authors sincerely thank the past and present Directors of CSIR–NAL for their unwavering encouragement and support. ❐

References

1. M. Mrazova, *Incas Bulletin* **5,** 139-150 (2013).
2. C. Soutis, *Progress in Aerospace Sciences* **41**, 143–151 (2005).
3. J. Zhang, G. Lin, U. Vaidya and H. Wang, *Composites Part B: Engineering* **250**, 110463 (2023).
4. M.O.W. Richardson and M.J. Wisheart, *Composites Part A: Applied Science and Manufacturing* **27**, 12 (1996).
5. P.J. Schilling, B.R. Karedla, A. Tatiparthi, M.A. Verges and P.D. Herrington, *Composites Science and Technology* **65**, 2071–2078 (2005).
6. T.K. Tan, N. Watanabe and Y. Iwahori, *Composites Part B: Engineering* **42**, 874–884 (2011).
7. Y. Gong, J. Luo, H. Shao and Z. Li, *Composite Structures* **284**, 115136 (2022).
8. Y. Nikishkov, L. Airoldi and A. Makeev, *Composites Science and Technology* **89**, 89–97 (2013).
9. L. Ping et al., *NDT and E International* **64**, 52–58 (2014).
10. R.A. Badcock and G.F. Fernando, *Smart Materials and Structures*, **4**, 223–230 (1999).
11. A. Datta et al., *International Conference on Fibre Optics and Photonics* (M3C-4), Optica Publishing Group (2014).
12. A. Datta et al., *Optical Fiber Technology* **66**, 102651 (2012).
13. Z. Lu, Q. Zhang and X. Liu, *Proceedings of the Fourth International Conference on Intelligent Systems Design and Engineering Applications*, IEEE, 403–406 (2013).
14. L. Toubal, M. Karama and B. Lorrain, *International Journal of Fatigue* **28**, 1867–1872 (2006).
15. H.S. Park, M.Y. Choi and J.H. Park, *Journal of the Korean Society for Nondestructive Testing* **31**, 150–156 (2011).
16. A. Rani and R. Mulaveesala, *Composite Structures* **286**, 115338 (2022).
17. S. Tuli and R. Mulaveesala, *Quantitative InfraRed Thermography Journal* **2**, 41–54 (2005).
18. K. Imielinska, M. Castaings and R. Wojtyra, *Journal of Materials Processing Technology* **157**, 513–522 (2004).
19. M. Cacciola, S. Calcagno and F.C. Morabito, *IEEE Transactions on Ultrasonics, Ferroelectrics, and Frequency Control* **55**, 870–878 (2008).
20. V.A. Kramb, R. John and D.A. Stubbs, *Composites Science and Technology* **61**, 1561–1570 (2001).
21. E. La Malfa Ribolla, M. Rezaee Hajidehi, P. Rizzo, G. Fileccia Scimemi, A. Spada and G. Giambanco, *Structure and Infrastructure Engineering* **14**, 807–816 (2018).
22. D. Pagodinas, *Ultragarsas/Ultrasound* 45, 47–54 (2002).
23. C. Scarponi and G. Briotti , *Journal of Reinforced Plastics and Composites* **16**, 768–790 (1997).
24. Y. Zhou, B. Ye, H. Cao, Y. Zou, Z. Zhu and H. Xing, *Applied Sciences* **14**, 3765 (2024).
25. A.J. Mohamad, K. Ali, D. Rifai, Z. Salleh and A.A.Z. Othman, *Journal of Physics: Conference Series* **2467**, 012030 (2023).

26. A. Sophian and A. Ali, *Insight* **43**, 302–306 (2001).
27. K.M. Holford, R. Pullin, S.L. Evans, M.J. Eaton, J. Hensman and K. Worden, *Proceedings of the Institution of Mechanical Engineers, Part G: Journal of Aerospace Engineering* **223**, 525–532 (2009).
28. H. Asemani, J. Park, J.R. Lee and N. Soltani, *Review of Scientific Instruments* **88**, 5 (2017).
29. H. Yang, L. Yang, Z. Yang, Y. Shan, H. Gu, J. Ma and Z. Wu, *Composite Structures* **324**, 117554 (2023).
30. M.E. Torbali, A. Zolotas and N.P. Avdelidis, *Applied Sciences* **13**, 2732 (2023).
31. S. Han, Q. Li, Z. Cui, P. Xiao, Y. Miao, L. Chen and Y. Li, *Nondestructive Testing and Evaluation* **39**, 725-761 (2024).
32. B.W. Drinkwater and P.D. Wilcox, *NDT & E International* **39**, 525–541 (2006).
33. https://sonatestap.com/SoftwareUpdates/RapidScan/Obsolete/rs2_manual.pdf (accessed on 08-05-2024).
34. https://scanmaster-irt.com/wp-content/uploads/2015/08/Squirter-based-Inspection-systems-New Address.pdf (accessed on 08-05-2024).
35. https://ultrangroup.com/wp-content/uploads/transducer-catalog.pdf (accessed on 08-05-2024).
36. A. Wronkowicz, A. Katunin and K. Dragan, *International Journal of Image, Graphics, and Signal Processing* **7**, 1-8 (2015).
37. A. Wronkowicz and K. Dragan, *Composites Theory and Practice* **16**, 154-160 (2016).
38. S. Liu, F. Liu, Y. Yang, L. Li and Z. Li, *Research in Nondestructive Evaluation* **31**, 370–388 (2020).
39. S. Cantero-Chinchilla, P.D. Wilcox and A.J. Croxford, *NDT and E International* **131**, 102703 (2022).
40. A. Datta et al., *Journal of Non-Destructive Testing and Evaluation* **20**, 70–76 (2023).
41. I. Gray et al., *Proceedings of the 18th European Conference on Composite Materials*, Athens, Greece, 24–28 (2018).